Biochemical, Biophysical, and Pharmacological Characterization of Bacterially Expressed Human Agouti-Related Protein

ARTICLE *in* BIOCHEMISTRY · DECEMBER 1998

Impact Factor: 3.02 · DOI: 10.1021/bi981027m · Source: PubMed

Biochemical, Biophysical, and Pharmacological Characterization of Bacterially Expressed Human Agouti-Related Protein

Robert D. Rosenfeld, Lisa Zeni, Andrew A. Welcher, Linda O. Narhi, Clarence Hale, Julie Marasco, John Delaney, Thomas Gleason, John S. Philo, Viswanathan Katta, John Hui, Jamie Baumgartner, Melissa Graham, Kevin L. Stark, and William Karbon

Amgen Inc., One Amgen Center Drive, Thousand Oaks, California 91320-1789

Biochemistry®

Reprinted from
Volume 37, Number 46, Pages 16041–16052

Biochemical, Biophysical, and Pharmacological Characterization of Bacterially Expressed Human Agouti-Related Protein

Robert D. Rosenfeld,* Lisa Zeni, Andrew A. Welcher, Linda O. Narhi, Clarence Hale, Julie Marasco, John Delaney, Thomas Gleason, John S. Philo, Viswanathan Katta, John Hui, Jamie Baumgartner, Melissa Graham, Kevin L. Stark, and William Karbon

Amgen Inc., One Amgen Center Drive, Thousand Oaks, California 91320-1789

Received May 5, 1998; Revised Manuscript Received August 6, 1998

ABSTRACT: The agouti-related protein gene (*Agrp*) is a novel gene implicated in the control of feeding behavior. The hypothalamic expression of *Agrp* is regulated by leptin, and overexpression of *Agrp* in transgenic animals results in obesity and diabetes. By analogy with the known actions of agouti, these data suggest a role for the *Agrp* gene product in the regulation of melanocortin receptors expressed in the central nervous system. The availability of recombinant, highly purified protein is required to fully address this potential interaction. A nearly full-length form of AGRP (MKd5-AGRP) was expressed in the cytosolic or soluble fraction of *Escherichia coli* and appeared as large intermolecular disulfide-bonded aggregates. Following oxidation, refolding, and purification, this protein was soluble, and eluted as a single symmetric peak on RP-HPLC. Circular dichroism studies indicated that the purified protein contains primarily random coil and β-sheet secondary structure. Sedimentation velocity studies at neutral pH demonstrated that MKd5-AGRP is monomeric at low micromolar concentrations. Mobility shifts observed using SDS−PAGE under reducing and nonreducing conditions for bacterially expressed and mammalian expressed AGRP were identical, an indication of a similar disulfide structure. The purification to homogeneity of a second, truncated form of AGRP (Md65-AGRP) which was expressed in the insoluble or inclusion body fraction is also described. Both forms act as competitive antagonists of α-melanocyte stimulating hormone (α-MSH) at melanocortin-3 (MC-3) and melanocortin-4 receptors (MC-4). The demonstration that AGRP is an endogenous antagonist with respect to these receptors is a unique mechanism within the central nervous system, and has important implications in the control of feeding.

The molecular and biochemical analysis of mouse mutants has identified a number of genes involved in obesity, such as *leptin* (*1*), the carboxypeptidase E gene (*2*), and *tubby* (*3*, *4*). One of the earliest mutants studied was mice (named *yellow*, A^y) in which a spontaneous mutation occurred within the *agouti* locus (*5*), resulting in the phenotype of a yellow coat color, pronounced obesity, and diabetes as well as a propensity to develop tumors (*6*). The molecular cloning of the *agouti* gene allowed the first molecular and biochemical analysis of this obese phenotype. The gene is predicted to encode a secreted, 131-amino protein which is normally expressed in the skin of the animal. As a result of a chromosomal deletion in the A^y mouse, the agouti gene is inappropriately expressed in all tissues of the mouse, including the brain (*7*). Further studies (*8*) showed that agouti protein acted as a competitive antagonist at the melanocortin-1 receptor (MC-1), preventing the binding of the ligand α-melanocyte stimulating hormone (α-MSH[1]). Thus, the pigmentation produced by the melanocyte depends on the relative occupancy of the MC-1 by either the ligand (α-MSH) or the antagonist (agouti).

Since the MC-1 and agouti are normally expressed only in the skin, the obese phenotype of the A^y mouse suggested that the ectopic expression of agouti might cause obesity by antagonizing one of the other four known melanocortin receptors. Direct evidence for the role of melanocortin receptor-4 (MC-4) was obtained by biochemical, pharmacological, and genetic methods. Recombinant agouti protein produced from a baculovirus system was found to be a potent antagonist of the centrally expressed MC-4 (*8*). Central administration of either an agonist or an antagonist for the MC-3 and MC-4 inhibited or stimulated food intake in mice, respectively (*9*). Finally, deletion of the MC-4 in mice resulted in an obese and diabetic phenotype (*10*). These data implied the existence of a gene related to agouti which would normally be expressed in the brain.

A gene related to agouti has recently been described (*11*) and was originally named agouti-related transcript (ART, *Agrt*). To ensure clarity between the gene and protein nomenclature, we have changed the gene name to *Agrp*, and the protein is designated AGRP. In situ analysis of mouse

* To whom correspondence should be addressed. Telephone: (805) 447-2430. Fax: (805) 499-7464. E-mail: robertr@amgen.com.

[1] Abbreviations: *Agrt*, agouti-related transcript; AGRP, agouti-related protein; MKd5-AGRP, methionine-lysine des 5 AGRP; α-MSH, α-melanocyte stimulating hormone; NDP-α-MSH, [Nle^4,D-Phe^7]-α-melanocyte stimulating hormone; CD, circular dichroism; TFA, trifluoroacetic acid; RP-HPLC, reversed phase high-performance liquid chromatography; MALDI, matrix-assisted laser desorption ionization; PBS, phosphate-buffered saline; SDS−PAGE, sodium dodecyl sulfate−polyacrylamide gel electrophoresis; DTT, dithiothreitol; PCR, polymerase chain reaction; HEK 293 cells, human embryonic kidney 293 cells; DMEM, Dulbecco's Modified Eagle's Media; FBS, fetal bovine serum; PSG, penicillin/streptomycin/glutamine.

10.1021/bi981027m CCC: $15.00
Published on Web 10/29/1998

Table 1: Sequence of Human MKd5-AGRP Where the Numbering Is Based on the Predicted Secreted Molecule[a]

-2	6	10	20	30	40	50
M	K	APMEGIRRPDQALLPELPGLGLRAPLKKTTAEQAEEDLLQEAQALAEVLDLQDR				

60	70	80	90	100	110
EPRSSRRCVRLHESCLGQQVPCCDPCATCYCRFFNAFCYCRKLGTAMNPCSRT					

[a] The sequence AQMGL is the first five amino acids of the predicted secreted protein missing from the form expressed.

tissues showed a strikingly restricted expression pattern in the arcuate nucleus of the hypothalamus, a brain region long known to regulate food intake. This hypothalamic expression is upregulated about 10-fold in mice lacking leptin (*ob/ob*) or the leptin receptor (*db/db*). *Agrp* encodes a 132-amino acid protein with a putative 20-amino acid secretion signal, and is 25% identical to human agouti. Both agouti and AGRP contain ten cysteines in the secreted molecule, nine of which are spatially conserved. Transgenic mice ectopically overexpressing *Agrp* were obese and diabetic (*12*, *13*), directly implicating this gene in the control of food intake. By analogy with agouti, AGRP would be predicted to have activity at the centrally expressed melanocortin receptors-3 and -4. Recently, two groups have provided partial evidence for such activity using either unpurified conditioned medium from COS cells (*14*) or partially purified proteins from a baculovirus expression system (*13*).

In this study, two forms of human AGRP were expressed using a bacterial system and subsequently refolded and purified to homogeneity. One form, expressed as methionine-lysine des 5 AGRP (MKd5-AGRP), was present in the cytosolic fraction of an *Escherichia coli* lysate and appeared as large intermolecular disulfide-bonded aggregates. A second form containing the 47 amino acids of the C-terminal domain of human AGRP (Md65-AGRP) was expressed in the insoluble or inclusion body fraction. These forms once refolded and purified were used to further characterize the biochemical, biophysical, and pharmacological properties of AGRP.

EXPERIMENTAL PROCEDURES

Expression and Fermentation Conditions for MKd5-AGRP and Md65-AGRP Expression in E. coli. Two PCR fragments encoding truncations of 5 and 65 codons from the 5′-end of the predicted secreted form of human AGRP were generated using Taq polymerase (Perkin-Elmer) or Advantage-GC kit (Clontech), respectively. The templates used in each case were plasmids encoding the human AGRP cDNA. For the des 5 construct, an additional lysine codon was inserted immediately 3′ to the initiating methionine codon. The oligonucleotides utilized for amplification were as follows: MKd5-AGRP (5′-primer), 5′-CATATGAAAGCCCCCATGGAGGGCATCAGA-3′; MK des 5-AGRP (3′-primer), 5′-GAATTCTTAGGTGCGGCTGCAGGGATTCAT-3′; Md65-AGRP (5′-primer), 5′-AGGTTTGGTTAACATATGCGCTGCGTAAGGCTGCAT-3′; and Md65-AGRP (3′-primer), 5′-ATCTTAATTGAATTCTTAGGTGCGGCTGCAGGGATTCAT-3′. Subcloning of the des 5 gene was carried out in the T/A cloning vector pCR2.1 (Invitrogen). Digestion of the resulting plasmid with *Nde*I and *Eco*RI (New England Biolabs) released a fragment of 326 bp which was isolated (QIAquick gel extraction kit, Qiagen) and ligated (T4 DNA ligase, New England Biolabs) with an *Nde*I−*Eco*RI-linearized *E. coli* expression plasmid. The des 65 PCR fragment was digested with *Nde*I−*Eco*RI and ligated directly into the same *Nde*I−*Eco*RI-linearized expression vector. A prototroph was used as the host for both plasmids, generating strains for inducible, temperature-independent expression of the AGRP truncations. Fermentations were performed on the 10 L scale using an N-Z amine-based (Quest) complex media employing glycerol as the carbon source. Both fermentations were carried out at 30 °C.

Oxidation, Refolding, and Purification of MKd5-AGRP. Attempts to express the full-length secreted form of AGRP were unsuccessful. A synthetic gene encoding a form of human AGRP missing (des) the first five amino acids of the predicted secreted protein (Table 1) was expressed with an additional amino-terminal lysine. Expression of this form in *E. coli* led to the production of met-lys des 5 AGRP (MKd5-AGRP). Wet cells (about 1340 g) from 10 L of culture broth were stored at −80 °C in portions (320 g). A portion (320 g) was resuspended in 5 volumes (1.6 L) of ice-cold water containing 10 mM benzamidine hydrochloride and lysed at 16 000 psi using a microfluidizer, and the resulting lysate was centrifuged for 30 min at 10000*g*. MKd5-AGRP was detected only in the soluble fraction. Guanidine hydrochloride and sodium phosphate (pH 7.0) were added such that final concentrations of 6 M guanidine and 10 mM phosphate were obtained, and the mixture was allowed to stir at room temperature for 2 h. The denatured soluble fraction (3 L) was then diluted 10-fold over the course of 2 h into 30 L of ice-cold oxidation/refold buffer containing Tris-HCl (pH 9.0), 1 M urea, and a redox couple (3 mM L-cysteine/0.3 mM cystamine dihydrochloride). The solution was kept at 4 °C for 20 h. The solution was then concentrated and buffer exchanged versus 10 mM sodium phosphate (pH 7.0) containing 2 M urea, using two Amicon S10/Y10 cartridges in series, and then clarified by centrifugation and applied to a Pharmacia SP-Sepharose fast flow (7 cm × 10 cm) column equilibrated in sodium phosphate (pH 7.0) at 4 °C. After the sample application and a 10 column volume wash with equilibration buffer, the column was eluted stepwise with an increasing level of sodium chloride in the same buffer. AGRP eluted with 0.1 M NaCl.

This eluate was then adjusted to pH 5.2 with acetic acid and allowed to sit at 4 °C overnight. The solution was then clarified by centrifugation, adjusted to pH 8.0, and then concentrated and buffer exchanged against Tris buffer (pH 8.5), using an Amicon S10/Y10 cartridge. This solution was then applied to a Q-Sepharose fast flow (4.4 cm × 15 cm) column equilibrated in 10 mM Tris buffer (pH 8.5) at 4 °C. After the sample application and a 10 column volume wash with equilibration buffer, the bound protein was eluted with a 30 column volume linear sodium chloride gradient in the same buffer. AGRP eluted around 30 mM NaCl. As a final chromatography and concentration step, the pH of the Q-Sepharose pool was adjusted to pH 5.0 with acetic acid and the mixture applied directly to an SP-Sepharose high-performance column at 4 °C (1.6 cm × 5 cm) equilibrated in sodium acetate (pH 5.0). After the sample application and a 10 column volume wash with equilibration buffer, the column was re-equilibrated with 10 mM sodium phosphate (pH 7.0) followed by increasing steps of NaCl in the same buffer. MKd5-AGRP was eluted using 150 mM NaCl in phosphate buffer (PBS) and was then sterile filtered using a 0.22 μm membrane and stored in aliquots at 4 °C.

Oxidation, Refolding, and Purification of Md65-AGRP. Wet cells (about 365 g) from a 10 L *E. coli* fermentation mixture expressing a synthetic gene missing the first 65 amino acids of the predicted secreted form of human AGRP (Md65-AGRP) were stored at −80 °C in portions. Wet cells (about 170 g) were resuspended in 10 volumes (1.7 L) of ice-cold water containing 5 mM benzamidine hydrochloride and lysed at 16 000 psi using a microfluidizer. The resulting lysate was centrifuged for 30 min at 10000*g*. Md65-AGRP was detected in the insoluble fraction or inclusion bodies. This material (about 25 g) was resuspended in ice-cold water containing 1% deoxycholic acid, homogenized, and centrifuged at 10000*g* for 30 min. The resulting pellet (about 24 g) was resuspended in 240 mL of ice-cold water, homogenized, and centrifuged at 10000*g* for 30 min. The resulting 22 g of washed inclusion bodies containing all the detectable Md65-AGRP was resuspended in a reducing denaturing buffer containing 10 mM sodium phosphate, 6 M guanidine hydrochloride, and 5 mM dithiothreitol (DTT) at pH 7.0 and the mixture allowed to stir at room temperature for 1.5 h followed by centrifugation at 10000*g* for 60 min. The solution of 220 mL was added slowly over the course of 2 h to 30 volumes (6.6 L) of an oxidation and refolding buffer containing Tris buffer (pH 9.8), 1 M urea, and a redox couple (3 mM L-cysteine/0.3 mM cystamine dihydrochloride) at 4 °C. The refolding was allowed to proceed for 20 h at 4 °C. After 20 h, sodium acetate was added and the solution was titrated with glacial acetic acid to pH 4.5. The solution (conductivity measuring about 17 mS/cm) was clarified by centrifugation at 10000*g* for 45 min and applied directly to an SP-Sepharose fast flow column (4.4 cm × 19 cm) equilibrated in sodium acetate (pH 4.5) at 4 °C. The column was then washed with 10 column volumes of equilibration buffer, followed by 10 column volumes of sodium phosphate buffer (pH 7.0). The column was then eluted stepwise with an increasing level of sodium chloride in the same buffer. Md65-AGRP was detected in the 0.2 M NaCl eluate (1 L). This eluate was adjusted by adding sodium acetate to 10 mM and titrating to pH 5.0 with glacial acetic acid. Solid ammonium sulfate was then added slowly to 1 M at room temperature. The solution was clarified by centrifugation and applied to a Phenyl Sepharose high-performance column (1.6 cm × 5 cm) equilibrated in sodium acetate and 1 M ammonium sulfate (pH 5.0) at room temperature. The column was then washed with 10 column volumes of equilibration buffer and then eluted with a 20 column volume linear gradient with a decreasing level of ammonium sulfate in the same buffer. Md65-AGRP eluted at about 0.4 M ammonium sulfate. This eluate was subsequently buffer exchanged into PBS and stored in aliquots at 4 °C.

Mass Spectral Analysis. Recombinant AGRP samples were analyzed using a matrix-assisted laser desorption ionization (MALDI) time-of-flight mass spectrometer (Voyager DERP, Perseptive Biosystems Inc., Framingham, MA). The instrument was operated in a linear mode (25 kV acceleration, 90% grid, 0.1% guide wire, and 500 MHz digitizer) and employed delayed extraction (150 ns). The *m/z* scale was externally calibrated using a mixture of known protein samples. Samples (1−10 pmol) were mixed with either a saturated solution of sinapinic acid or 4-hydroxy-α-cyanocinnamic acid matrix mixed (1:1 v/v) with acetonitrile containing 0.1% trifluoroacetic acid. The samples were deposited on the probe, air-dried, and inserted into the mass spectrometer. Spectra arising from 50−100 laser shots were averaged, and a 19-point smoothing of data was utilized for protein samples.

N-Terminal Sequencing. Automated Edman degradation of proteins was carried out using an Applied Biosystems sequencer (model 477A, Foster City, CA), with an on-line HPLC analyzer for the identification of phenylthiohydantoin (PTH) amino acids.

Preparation of the Antiserum. Three New Zealand white rabbits were hyperimmunized over a period of 4 months with recombinant human MKd5-AGRP, covalently coupled to keyhole limpet hemocyanin serving as the immunogen. After 4 months of boosting and monitoring, anti-MKd5-AGRP titers of test bleeds revealed moderate antibody titers in all three rabbit antisera. Production bleeds of about 50 mL were obtained from each animal. Rabbit antisera served as the antibody source for Western blots.

Electrophoresis and Western Blotting. Electrophoresis was performed according to standard methods (*15*) with the exception that the reducing agent was in some cases omitted from the sample buffer. Precast 16 or 18% gels were used (Novex, Encinitas, CA). Immunoblots of SDS gels were prepared according to standard methods (*16*) except that 5% nonfat milk was used to block binding sites on the nitrocellulose after protein transfer. All washes were carried out in PBS containing 0.1% Tween 20. For development of the blots, the nitrocellulose was treated with a dilution of antiserum against MKd5-AGRP. The secondary antibody was donkey anti-rabbit IgG coupled to horseradish peroxidase (Amersham), and bound antibody was detected by chemiluminescence (ECL, Amersham).

Sedimentation Velocity. Sedimentation velocity experiments were carried out in PBS at 20 °C using dual-channel charcoal-Epon cells in a Beckman XL-A analytical ultracentrifuge. Fitting of these data to determine sedimentation coefficients and molecular mass was achieved using the program SVEDBERG (*17*). Calculation of partial specific volumes and frictional coefficients was done with the

program SEDNTERP, using anhydrous radii calculated by the Teller method and a calculated hydration of 0.39 g/g (*18*).

Circular Dichroism (CD). The CD spectra were recorded on a Jasco J-715 spectropolarimeter. Cuvettes with a path length of 0.02 cm were used for the far-UV CD spectra (secondary structure, 250−190 nm), while cuvettes with a 1 cm path length were used for the near-UV CD region (tertiary structure, 340−240 nm). Analyses were performed at ambient temperature in PBS. Thermally induced denaturation was performed on a Jasco J-720 spectropolarimeter equipped with a Peltier JTC-345 thermal control unit, using rectangular cuvettes with a 0.1 cm path length. Spectra were collected every 2 °C, as the temperature was increased from 24 to 86 °C at a rate of 20 °C/h.

Reversed Phase HPLC. Reversed phase HPLC (RP-HPLC) was employed using a Waters 625 solvent delivery module, a 715 autosampler, and a Hewlett-Packard 1040M diode array detector with an HP Chemstation for data acquisition. The following buffers were used to develop gradients for elution: buffer A (0.1% trifluoroacetic acid in water) and buffer B (90% acetonitrile, 0.1% trifluoroacetic acid, and 9.9% water). The samples were analyzed using a Vydac C4 reversed phase column, 214TP54 (0.46 cm × 25 cm). The column was heated to 60 °C using a column heater with a digital temperature controller, to improve the reproducibility of peak areas and elution times.

HPLC−Gel Filtration Chromatography. A convenient technique for the determination of protein molecular size and detection of multimeric forms in solution is gel filtration chromatography. A Superose 12 HR 10/30 gel filtration column (Pharmacia) was equilibrated in 50 mM sodium phosphate containing 500 mM sodium chloride (pH 7.0). The elution volume of MKd5-AGRP was compared to those measured for protein standards. From this analysis, an apparent molecular mass can be determined for the protein of interest.

Protein Determination. The total protein was determined throughout the experiments using a Coomassie dye binding reagent on the basis of the method of Bradford (*19*). Theoretical extinction coefficients (A_{280}[0.1%,1 cm]) of 3.00 and 6.62 were calculated for MKd5-AGRP and Md65-AGRP, respectively. The final purified products were then used to generate standard curves using RP-HPLC, plotting peak area for the peak of interest versus the number of micrograms injected. In this way, the amount of AGRP in crude samples could be determined with the peak area.

Analysis of Free Protein Thiol. Analysis of free protein thiol was carried out using 5,5′-dithiobis(2-nitrobenzoic acid) (DTNB) according to the method of Ellman (*20*), except that 6 M guanidine hydrochloride was included in the assay buffer to promote side chain availability.

Expression of AGRP in AtT20 Cells. AtT20 cells were cultured in 95% humidified air and 5% CO_2 at 37 °C. Cells were maintained in DMEM supplemented with nonessential amino acids, 2 mM L-glutamine, and 10% fetal bovine serum. The human AGRP expression vector pCDNA Hu AGRP was constructed by subcloning a 400 bp *Eco*RI restriction fragment containing the human AGRP cDNA sequence into the vector pCDNA (Invitrogen). The orientation of the sequence was confirmed by DNA sequencing.

Transient Transfection in AtT20 Cells. AtT20 cells were transiently transfected with the construct pCDNA Hu AGRP or with the pCDNA vector using the transfection reagent Lipofectamine PLUS (Life Technologies). The day before transfection, cells were trypsinized and plated at a density of 0.8 × 10^6/6 cm dish. The following day, 4 μg of pCDNAHuAGRP, 8 μL of PLUS reagent, and 20 μL of Lipofectamine were complexed (according to the manufacturer's instructions). The complex was then diluted with 2 mL of serum free DMEM and the mixture added to AtT20 cells from which the media had been removed. The cells were incubated with the transfection mix for 5 h at 37 °C, and then the mix was diluted to 5 mL with 2× complete media and incubated overnight. The following morning, the transfection mixture was replaced with 2.5 mL of complete media containing 0.5% fetal bovine serum and incubated for an additional 24 h. The media were removed from the transfected cells, filtered, and then stored −80 °C. Detection of AGRP by Western blot required the media to be concentrated 10-fold using a Centricon 3 instrument (3000 Da molecular mass cutoff) prior to loading an aliquot for SDS−PAGE analysis.

MC-3 and MC-4 Binding. Human embryonic kidney (HEK) 293 cells stably expressing human MC-3 or MC-4 were used for radioligand binding studies. Cells were maintained in DMEM containing 10% FBS, penicillin/streptomycin/glutamine (PSG), and G418 (50 μg/mL) at 37 °C in a humidified environment of 95% O_2/5% CO_2. Cells were collected in PBS and homogenized in buffer A containing 25 mM HEPES and 0.32 M sucrose (pH 7.4), after which the homogenate was spun at 48000*g* for 12 min. The resulting pellet was resuspended in buffer B containing 25 mM HEPES, MEM (without phenol red), 0.1% BSA, 0.1 mg/mL soybean trypsin inhibitor, and 0.1 mg/mL AEBSF (pH 7.4), and the mixture was spun at 48000*g* for 12 min. This step was repeated one additional time, and the final pellet was resuspended in buffer B to a tissue concentration of 4 mg of wet weight/mL.

The binding reaction was initiated by the addition of tissue homogenate (50 μL) to wells containing 0.15 nM [^{125}I]NDP-α-MSH (2000 Ci/mmol, Amersham) and varying concentrations of displacing agent. The final assay volume was 100 μL. Previous studies in our laboratory demonstrated that equilibrium binding was achieved with an incubtaion time of 180 min. Accordingly, the reaction mixture was incubated for 180 min at 25 °C and the reaction terminated by filtration over Unifilter 96 glass fiber filter plates that had been presoaked in 0.1% polyethylenimine (PEI). Filters were rinsed with ice-cold H_2O, followed by the addition of 37 μL of Packard MicroScint to each filter well. Radioactivity was quantified using a Packard TopCount. Each concentration of displacing agent was tested in triplicate. Specific binding was defined as that portion of total binding that could be displaced by 1 μM unlabeled NDP-α-MSH and was typically greater than 80%. The concentration of test compound producing a 50% reduction in specific binding (IC_{50}) was determined using nonlinear regression analysis (Graphpad PRIZM).

Cyclic AMP Assay. MKd5-AGRP and Md65-AGRP were tested for their ability to inhibit α-MSH-stimulated cyclic AMP production in CHO K1 cells stably expressing either MC-3 or MC-4. Each cell line was stably transfected with a reporter construct consisting of a cyclic AMP response element coupled to a luciferase gene, and cyclic AMP

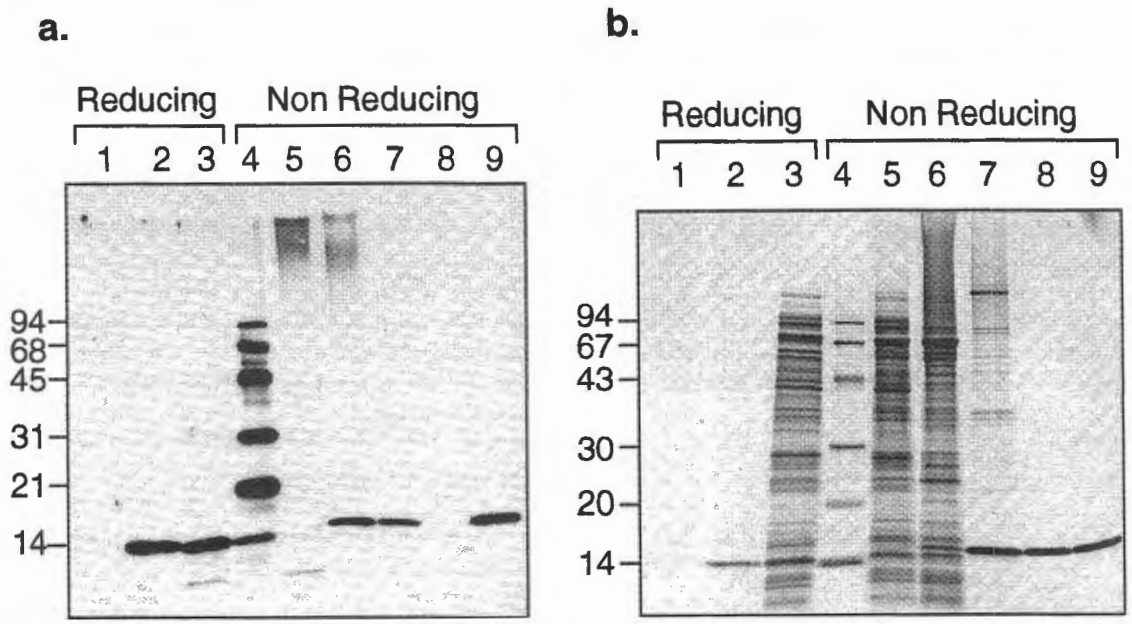

FIGURE 1: Analysis of MKd5-AGRP before and after refolding and purification using 16% SDS−polyacrylamide gels. (a) Western blot analysis: lanes 1−3, reducing conditions; lanes 4−9, nonreducing conditions; buffer blank (lane 1); 2 ng of MKd5-AGRP (lane 2); soluble fraction (lane 3); Bio-Rad's biotinylated SDS−PAGE standards [phosphorylase B (97 kDa), bovine serum albumin (68 kDa), ovalbumin (45 kDa), carbonic anhydrase (31 kDa), soybean trypsin inhibitor (21 kDa), and lysozyme (-14 kDa)] (lane 4); soluble fraction (lane 5); soluble fraction after oxidation and refolding (lane 6); SP-Sepharose pool (lane 7); buffer blank (lane 8); 2 ng of the MKd5-AGRP purified standard (lane 9). (b) Coomassie blue stain analysis: lanes 1−3, reducing conditions; lanes 4−9, nonreducing conditions; buffer blank (lane 1); 0.5 μg of the Mkd5-AGRP standard (lane 2); soluble fraction (lane 3); Pharmacia carboxymethylated low-molecular mass electrophoresis standards [phosphorylase B (94 kDa), bovine serum albumin (67 kDa), ovalbumin (43 kDa), carbonic anhydrase (30 kDa), soybean trypsin inhibitor (20 kDa), and α-lactalbumin (14 kDa)] (lane 4); soluble fraction (lane 5); soluble fraction after oxidation and refolding (lane 6); SP-Sepharose pool and 1 μg of AGRP (lane 7); Q-Sepharose pool and 1 μg of AGRP (lane 8); S-Sepharose HP pool and 1 μg of AGRP (lane 9).

production was indirectly quantified by the extent of luciferase activity in the cell lysate. On the morning of day 1, cells were plated at a density of 4−5 × 10^5 cells/well in 96-well culture plates and the plates maintained at 37 °C in a humidified environment of 95% O_2/5% CO_2 in Ham's F12 media containing 10% FBS, PSG, and G418 (500 μg/mL). On day 2, the media were removed and replaced with serum-free media, and on day 3, the serum-free media were removed and replaced with incubation buffer consisting of Ham's F12 media, 0.1 mM isobutylmethylxanthine, 0.1% BSA, and PSG. Experiments for determining dose responses to α-MSH were performed in the presence of either vehicle or a fixed concentration of MKd5 or Md65-AGRP. Test compounds were added to triplicate wells, and plates were returned to the incubator for a period of 8 h, after which the media were removed and replaced with 100 μL of PBS. The PBS was removed, and 100 μL of lysis buffer (Promega) was added to each well. Luciferase activity, defined as relative luciferase units (RLU), was detected using a Promega assay kit and quantified using a Titertek Luminoscan (ICN). The concentration of α-MSH producing 50% of the maximal stimulation of luciferase activity (ED_{50}) was determined using nonlinear regression analysis (Graphpad PRIZM). These ED_{50} values were used to determine the dose ratio (i.e., the ratio of agonist concentrations producing a half-maximal response in the absence and presence of antagonist) for each antagonist concentration. pA_2 values were determined by linear regression analysis of Schild regression (*21*) in which log(dose ratio − 1) is plotted versus log[antagonist]. pA_2 is equal to $-\log K_{DB}$, where K_{DB} is defined as the equilibrium dissociation constant for the antagonist−receptor interaction.

RESULTS

Oxidation, Refolding, and Purification of MKd5-AGRP. Utilizing a bacterial expression system, MKd5-AGRP was expressed in the cytosolic fraction. Although the recombinant protein was soluble in aqueous solution, it appeared to be aggregated, and attempts to purify MKd5-AGRP directly from the soluble fraction were unsuccessful. An aliquot of the soluble fraction was applied to a Superose 12 gel filtration column at neutral pH, and fractions were collected. Detection of MKd5-AGRP from the gel filtration column fractions was performed by reducing SDS−PAGE followed by Coomassie blue stain. Interestingly, MKd5-AGRP was detected primarily in the void volume, indicating the material was aggregated in solution (data not shown). To determine if the mobility of MKd5-AGRP in the soluble fraction would change under reducing and nonreducing conditions, SDS−PAGE Western blot as well as Coomassie blue stain analysis was performed. When the soluble fraction was analyzed under reducing conditions, a discrete immunoreactive band was observed at about 14 kDa (Figure 1a, lane 3) that migrated in the same position as the 14 kDa lysozyme standard (Figure 1a, lane 4). To help confirm the identity of the immunoreactive band in the soluble fraction, a 2 ng aliquot of the MKd5-AGRP final product is also shown (Figure 1a, lane 2). When the soluble fraction was analyzed under nonreducing conditions, diffuse as well as discrete immunoreactive bands corresponding to a high molecular mass of >200 kDa were evident (Figure 1a, lane 5). On the basis of these observations, it became apparent that MKd5-AGRP in the soluble fraction was at least partially oxidized and appeared as intermolecular disulfide-linked

aggregates. The occurrence of a bacterially expressed protein in the cytosolic fraction which requires reoxidation and refolding is uncommon but not unique (*22*). To determine optimal conditions for reoxidizing and refolding recombinant human MKd5-AGRP, three techniques were employed. The first method involved SDS−PAGE with reducing and nonreducing conditions. A mobility shift of the band of interest is an indication of oxidation or disulfide formation (*23*). A second method involved RP-HPLC (*24*), which relied on monitoring elution time shifts of the peak of interest and was also used to quantitate the concentration of the recombinant protein during the process. Last, an aliquot of the sample was applied to a gel filtration column, and the peak elution volume was compared to those of protein molecular mass standards.

A refolding matrix was initiated to determine the optimal conditions that might yield fully oxidized, monomeric protein with the highest efficiency. The variables in the refolding matrix included denaturant concentration, redox couple, temperature, pH, cosolvents, and other additives such as amino acids and salts that might enhance refolding efficiency.

Following oxidation and refolding of MKd5-AGRP, Western blot analysis demonstrated the disappearance of the aggregate bands at 200 kDa, accompanied by the formation of a new band with a molecular mass of 16 kDa (Figure 1a, lanes 5 and 6). The oxidized protein exhibits an upward mobility shift relative to the reduced protein (Figure 1a, lanes 9 and 2). The upward mobility shift is somewhat unexpected in that oxidized proteins run under nonreducing conditions usually migrate faster than the corresponding reduced form (*25*). This same analysis was performed with SDS−PAGE Coomassie blue stain. The soluble fraction analyzed under reducing conditions (Figure 1b, lane 3) shows MKd5-AGRP migrating with about the same mobility as the 14 kDa α-lactalbumin standard (Figure 1b, lane 4). This same sample analyzed under nonreducing conditions still showed a band at about the same mobility (Figure 1b, lanes 5) but with lighter intensity than the corresponding reducing lane. This band is an *E. coli* contaminant which is not recognized by Western blot analysis (Figure 1a, lane 5). Upon oxidation and refolding of the soluble fraction, MKd5-AGRP migrated at about 16 kDa and was clearly seen as a newly formed band migrating above the *E. coli* contaminant (Figure 1b, lane 6). Constant 1 μg aliquots of MKd5-AGRP from the three chromatography pools obtained during the purification are also shown (Figure 1b, lanes 7−9).

When the soluble fraction was analyzed by RP-HPLC, there were no discrete peaks corresponding to reduced or oxidized MKd5-AGRP (Figure 2a). If the reductant dithiothreitol (DTT) was added to the soluble fraction in the presence of denaturant and the mixture reanalyzed, a new peak corresponding to the reduced monomer of MKd5-AGRP was evident (Figure 2b). This is in agreement with the SDS−PAGE analysis, indicating that MKd5-AGRP in the soluble fraction is in neither the reduced nor properly oxidized form, but rather exists as a partially oxidized intermolecular disulfide-linked aggregate that does not elute discretely from the reversed phase column. Upon refolding, a new peak eluting 1 min earlier than the reduced peak was observed (Figure 2c), an indication of disulfide formation. The final product purity was also determined by RP-HPLC analysis. A symmetrical peak with no contaminating peaks

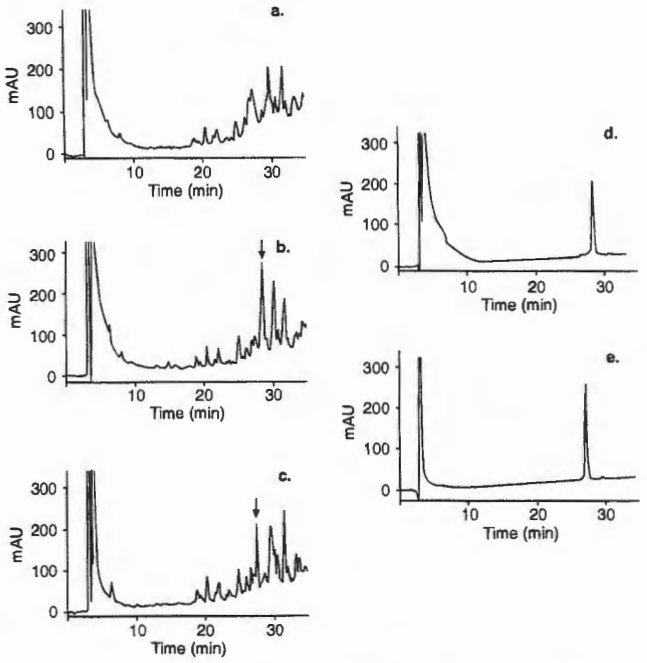

FIGURE 2: RP-HPLC analysis of MKd5-AGRP before and after oxidation and refolding. Samples were applied to a Vydac C4 reversed phase column (214 TP54, 4.6 mm × 250 mm) heated to 60 °C. The buffers used to develop the gradient for elution were buffer A (0.1% TFA in water) and buffer B (90% acetonitrile, 0.1% TFA, and 9.9% water). The column was equilibrated in 20% buffer B, and a gradient of 1% buffer B/min over the course of 35 min was used to elute bound proteins: (a) soluble fraction in 6 M guanidine hydrochloride, (b) soluble fraction in 6 M guanidine hydrochloride containing 0.1 M dithiothreitol, (c) soluble fraction after oxidation and refolding, (d) 5 μg of reduced MKd5-AGRP, and (e) 5 μg of the MKd5-AGRP final product.

Table 2: Purification of MKd5-AGRP[a]

step	volume (mL)	[protein] (mg/mL)	total protein[b] (mg)	[AGRP] (mg/mL)	total AGRP[c] (mg)	% recovery of AGRP
soluble fraction in 6 M guanidine	3000	10.00	30000	0.24	720	–
refolding mixture	33000	0.88	29040	0.01	430	60
SP Sepharose load	10000	2.60	26000	0.04	365	51
SP Sepharose 0.1 M eluate	3650	0.32	1170	0.08	274	38
Q Sepharose FF load	1750	0.25	440	0.09	153	22
Q Sepharose pool	1200	0.10	120	0.09	113	16
SP Sepharose pool	65	1.50	98	1.50	98	14

[a] A 10 L fermentation yields 1.3 kg of wet cell paste which yielded 6.5 L of soluble fraction. For these results, 1.6 L of soluble fraction was refolded and purified. [b] Total protein determined by Bradford (19). [c] Total AGRP determined by RP-HPLC peak area.

was observed, suggesting the final product does not contain multiple disulfide species (Figure 2e). The refolding efficiency based on RP-HPLC is 60%, yielding a 42-fold overall purification and an overall recovery of 14% (Table 2). The complete sequence of MKd5-AGRP (numbering based on the predicted secreted protein) is shown (Table 1).

Last, after the oxidation and refolding step, an aliquot was applied to a gel filtration column, and MKd5-AGRP migrated with an apparent molecular mass of about 12 kDa, indicating the material appeared to be monomeric in solution (data not shown).

Attempts to properly oxidize MKd5-AGRP directly in the soluble fraction, by raising the pH to 10, by adding copper

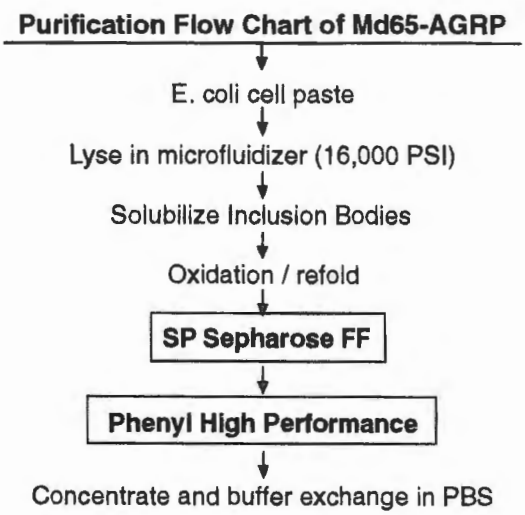

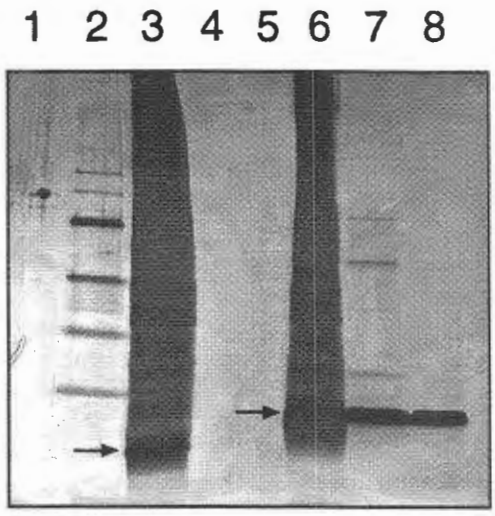

FIGURE 3: Purification flowchart of Md65-AGRP and 18% SDS−polyacrylamide gel electrophoresis silver stain analysis of serial steps of the refolding and purification of Md65-AGRP. A constant amount of Md65-AGRP (1 μg) from serial steps of the purification procedure was added to each lane: lanes 1−3, reducing conditions; lanes 4−8, nonreducing conditions; Pharmacia low-molecular mass electrophoresis standards, about 0.2 μg per standard (lane 2); solubilized inclusion bodies (lane 3); buffer blanks (lanes 4 and 5); refolding solution (lane 6); SP-Sepharose pool (lane 7); Phenyl Sepharose HP pool (lane 8).

sulfate as an oxidant, or by adding a redox couple, showed no evidence of the formation of the 16 kDa AGRP band (data not shown). This indicated that MKd5-AGRP in the soluble fraction required denaturation prior to refolding.

The final purified product was also assessed by SDS−PAGE silver stain analysis under reducing and nonreducing conditions which demonstrated a final product purity of ≥98% (data not shown).

Oxidation, Refolding, and Purification of Md65-AGRP. The isolation of Md65-AGRP from the insoluble fraction required solubilization in denaturant and reductant followed by dilution into an oxidation, refolding buffer. The complete process, described in Experimental Procedures, is illustrated with a flowchart as well as with a SDS−PAGE silver-stained gel (Figure 3). This C-terminal AGRP peptide displays the same upward mobility shift upon oxidation as that observed for MKd5-AGRP, but the shift is even more pronounced.

Analysis of the process used for the solubilization, oxidation, refolding, and purification of the C-terminal peptide was also performed by RP-HPLC. Chromatograms of the solubilized inclusion bodies as well as the peptide after oxidation and refolding are illustrated in Figure 4 (a and b). The purified C-terminal peptide displayed a symmetrical peak with no contaminating peaks, indicating the final purified product does not contain other disulfide variants (Figure 4c). The refolding efficiency based on RP-HPLC for Md65-AGRP is about 90% with an overall recovery of 60% (Table 3).

Free Thiol Analysis. To further assess the oxidation state of the purified AGRP proteins, the free thiol content was assayed. Free thiol could clearly be detected at a level of 0.09 mM. Ciliary neurotrophic factor (CNTF), which has one free cysteine, was included as a positive control, and the presence of a free cysteine at 2 mg/mL CNTF (0.09 mM) was clearly detectable and in the linear portion of the cysteine standard curve. MKd5-AGRP at a concentration of 3.3 mg/mL (0.27 mM) and Md65-AGRP at a concentration of 1.7 mg/mL (0.30 mM) had no detectable free thiols by this method. If either form of AGRP was missing one disulfide, the free cysteine concentration would be 0.54 and 0.6 mM, respectively. This would then imply that ≥83% of the MKd5-AGRP is fully oxidized and ≥85% of the Md65-AGRP is fully oxidized.

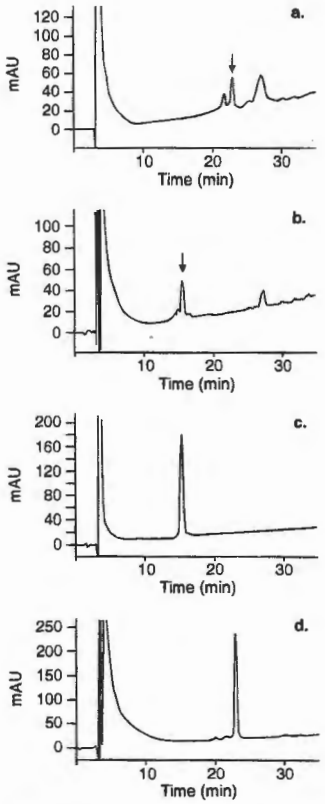

FIGURE 4: RP-HPLC analysis of Md65-AGRP before and after oxidation and refolding. Samples were applied to a Vydac C4 reversed phase column (214 TP54, 4.6 mm × 250 mm) heated to 60 °C. The buffers used to develop the gradient for elution were buffer A (0.1% TFA in water) and buffer B (90% acetonitrile, 0.1% TFA, and 9.9% water). The column was equilibrated in 20% buffer B, and a gradient of 1% buffer B/min over the course of 35 min was used to elute bound proteins: (a) solubilized inclusion bodies in 6 M guanidine hydrochloride and 5 mM dithiothreitol, (b) refold and oxidation pool, (c) 5 μg of the Md65-AGRP final product, and (d) 5 μg of reduced MKd5-AGRP.

Table 3: Purification of Md65-AGRP[a]

step	volume (mL)	[protein] (mg/mL)	total protein (mg)	[Md65-AGRP] (mg/mL)	total Md65-AGRP (mg)	% recovery AGRP
guanidine-solublized inclusion bodies	220	2.70	590	0.15	40	–
refolding mixture	6600	0.07	462	0.01	36	90
SP Sepharose pool	1000	0.05	50	0.04	32	80
Phenyl HP pool	57	0.43	24.5	0.43	24.5	61

[a] A 10 L fermentation yields 365 g of wet cell paste. For these results, 170 g of cell paste yielded 22 g of washed inclusion bodies.

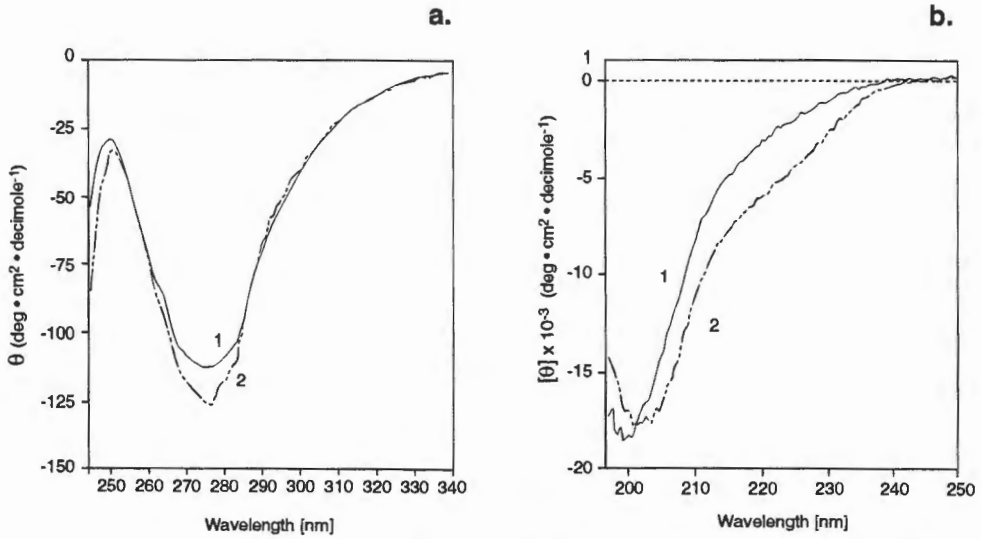

FIGURE 5: Circular dichroism spectra of MKd5-AGRP. (a) Near-UV CD spectra of AGRP at pH 7.2 (—, 1) and 2 (••—••, 2). Spectra are the average of 10 replicate scans recorded at 10 nm/min. (b) Far-UV CD spectra of AGRP at pH 7.2 (—, 1) and 2 (••—••, 2). Spectra are the average of 10 replicate scans recorded at 20 nm/min.

N-Terminal Sequencing. A 10 μL sample of MKd5-AGRP (1.5 mg/mL) was applied directly for N-terminal sequence. The sequence, MKAPMEGIRRPDQ... (initial yield of 950 pmol), was obtained with a second sequence KAPMEGIRR... (initial yield of 20 pmol). This indicates that about 2% of this material may be missing the amino-terminal methionine. No other sequences were detected.

A 10 μL sample of Md65-AGRP (0.9 mg/mL) was applied directly for N-terminal sequence analysis. The sequence MRXVRLHESXLGQ... (initial yield of 1.3 nmol) was obtained. No other sequences were detected. The cycles marked by X were expected to be cysteines, which could not be detected with this method.

Mass Spectral Analysis MALDI. The molecular masses of both forms of AGRP were measured using delayed extraction MALDI-TOF mass spectrometry. The measured values for the singly protonated species of *m/z* 12 218 (oxidized form) and 12 227.3 (reduced form) are within the mass accuracy (±0.03% typical) and are in close agreement with the theoretical values of *m/z* 12 222 (oxidized form) and 12 232 (reduced form). The increase in molecular mass of 9.3 Da upon reduction is consistent with the reduction of five disulfides (expected value of 10 Da), suggesting that all 10 cysteines were involved in disulfide bonds. Similar data were obtained in the case of oxidized and reduced forms of Md65-AGRP. The oxidized form showed singly protonated ions at *m/z* 5479.8 (theoretical value of 5479.5), and the reduced form showed a peak at *m/z* 5487 (theoretical value of 5489.5). The mass increase of 8 Da is less than the value of 10 Da expected for reduction of five disulfide bonds, probably due to incomplete reduction. The molecular masses measured correspond to average masses. To establish that all the cysteines in Md65-AGRP are involved in disulfides, the monoisotopic molecular mass was also measured using the high-resolution zoom scan mode with an electrospray ion trap mass spectrometer. The measured monoisotopic value of 5474.5 Da for the oxidized form is consistent with the theoretical value of 5474.3 Da and indicates five disulfide bonds were formed (data not shown).

Analysis of Structure (CD). CD studies were performed on MKd5-AGRP to examine the secondary and tertiary structure, as well as the thermal stability. The near-UV CD spectrum at pH 7.2 consists of a broad trough with a minimum at 275 nm and a maximum at 255 nm. This signal arises primarily from the disulfide bonds, and indicates that they are located in an asymmetric environment, which can only arise if the protein is folded into a defined three-dimensional conformation. At pH 2.0, the near-UV CD has the same shape, and a very similar intensity, demonstrating that the tertiary structure in the region surrounding the disulfide bonds is stable to acid pH (Figure 5a). Changes in tertiary structure with heat were determined by following changes at 275 and 253 nm as the temperature was slowly raised from 24 to 86 °C. There were no significant changes in the tertiary structure below 80 °C at protein concentrations of 0.19 and 1.9 mg/mL, while above 80 °C, the signal slowly disappears, indicating that the protein does not begin to unfold until temperatures of ≥80 °C are reached. The near-UV CD spectrum of the d65-AGRP analogue accounted for all of the signal seen in the MKd5-AGRP spectrum (data

not shown). This suggests that the N-terminal 65 amino acids are in a very flexible region of the protein, with little defined structure, while the remaining C-terminal region of the protein is folded into a well-defined three-dimensional structure. The far-UV CD spectra (Figure 5b) are consistent with a protein in which the secondary structure consists of almost equivalent amounts of random coil and distorted β-sheet structures, with about 10% β-turns (*26*). This is similar, but not identical, to the spectrum published for agouti (*27*). The spectrum at pH 2.0 is similar to that at pH 7.2, with a slight increase in intensity at 220−208 nm, and an increase in the intensity of the positive signal at 200 nm, consistent with the induction of a small amount of helix (less than 5%), and also an increase in the β-sheet content (by about 10%) with the equivalent decrease in random coil structure. This has been seen with other proteins as well (*28*, *29*). However, the slight changes in CD spectra seen with AGRP at pH 2 indicate that it maintains a structure very close to that of the native protein. It therefore can be classified as a type III protein, showing no significant unfolding as the pH is varied (*30*). Thermally induced denaturation of the secondary structure also occurs above 80 °C. When the protein is fully unfolded by the addition of danaturant, such as guanidine hydrochloride, the signals seen in the near-UV CD regions disappear, while the far-UV CD spectrum shifts to that of a protein containing only random coil structure.

Association State. Sedimentation velocity experiments in PBS at 270 and 50 μg/mL clearly indicated that MKd5-AGRP is monomeric at both concentrations, giving apparent molecular masses of 12.2 ± 0.3 kDa (data not shown). The sedimentation coefficient of 1.24 S implies a frictional coefficient relative to that of a sphere (f/f_o) of 1.55, which is much higher than expected for a compact globular protein. This high frictional coefficient would be consistent with a highly elongated, asymmetric molecular shape (axial ratio of 6.6 for a prolate ellipsoid), but alternatively could arise from large flexible loops or a disordered N- or C-terminal region. The fact that by gel filtration MKd5-AGRP elutes at its expected molecular mass favors the latter hypothesis. This is further supported by the finding that the near-UV CD spectrum of the d65 protein accounts for all the signal seen in the spectrum of MKd5-AGRP.

Expression of AGRP in AtT20 Cells. Many biologically active proteins are synthesized as inactive precursors and undergo limited proteolysis during processing to an active form. To determine if full-length AGRP was proteolytically processed, we examined the mobility of conditioned medium by SDS−PAGE Western blot analysis. We chose to express human AGRP in AtT20 cells, a murine pituitary cell line, because this cell line has a well-characterized, regulated secretory pathway which has been shown to correctly process bioactive proteins such as POMC (*31*), proinsulin (*32*), prorenin (*33*), and proneuropeptide-Y (*34*). When AtT20-conditioned medium was concentrated 10-fold and analyzed, the Western blot revealed that the mobility shift of *E. coli* expressed MKd5-AGRP and mammalian derived AtT20 AGRP is identical (Figure 7, lanes 1−3 reduced versus lanes 8−10 nonreduced). This is an indication that the disulfide structure is similar. In addition, when compared to the molecular mass standards as well as MKd5-AGRP, the major form of AGRP secreted from AtT20 cells appears to

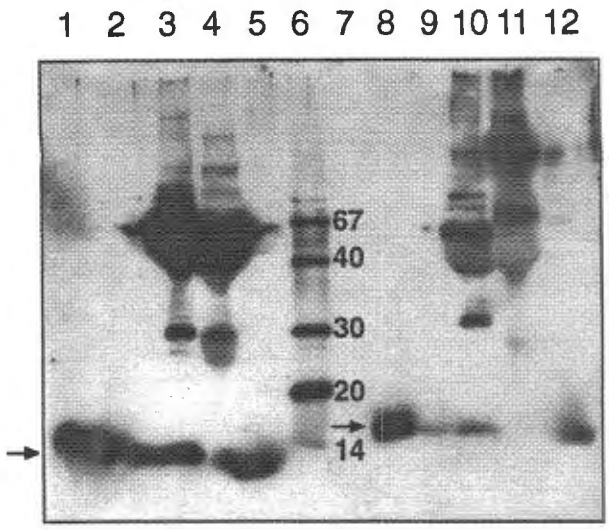

FIGURE 6: SDS−polyacrylamide gel electrophoresis (16%) Western blot analysis of AtT20 conditioned media. Lanes 1−6 were analyzed under reducing conditions, and lanes 7−12 were analyzed under nonreducing conditions: 1 ng of MKd5-AGRP (lane 1), 0.1 ng of MKd5-AGRP (lane 2), equivalent of 200 μL of AtT20 conditioned media (lane 3), equivalent of 200 μL of AtT20 conditioned media vector only negative control (lane 4), 1 ng of des28AGRP (lane 5), Bio-Rad's Biotinylated SDS−PAGE standards (lane 6), buffer blank (lane 7), 1 ng of MKd5-AGRP (lane 8), 0.1 ng of MKd5-AGRP (lane 9), equivalent of 200 μL of AtT20 conditioned media (lane 10), equivalent of 200 μL of AtT20 conditioned media vector only negative control (lane 11), and 1 ng of des28AGRP (lane 12).

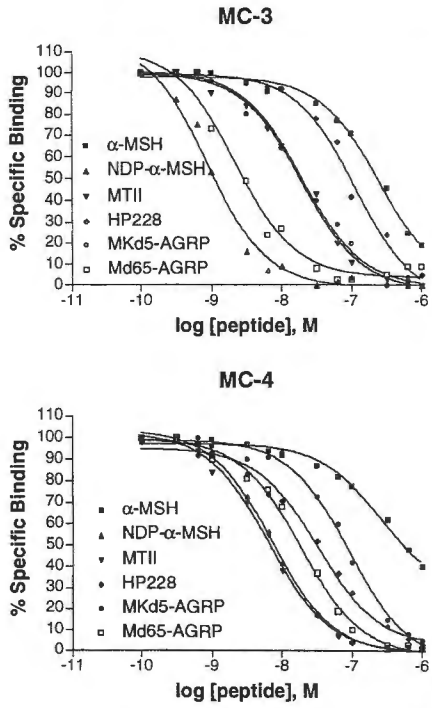

FIGURE 7: [^{125}I]NDP-α-MSH binding to MC-3 and MC-4 was achieved as described in Experimental Procedures. Specific binding was defined as that portion of total binding that could be displaced by excess, unlabeled NDP-α-MSH. Each point represents the mean of two separate experiments, with each experiment being performed using triplicate determinations.

correspond to the full-length form and does not show evidence of truncated forms. The antibody is more sensitive to detecting the reduced form over the oxidized form (lanes 1−5 vs 7−12). Although the antibody generated against MKd5-AGRP does not recognize the C-terminal peptide

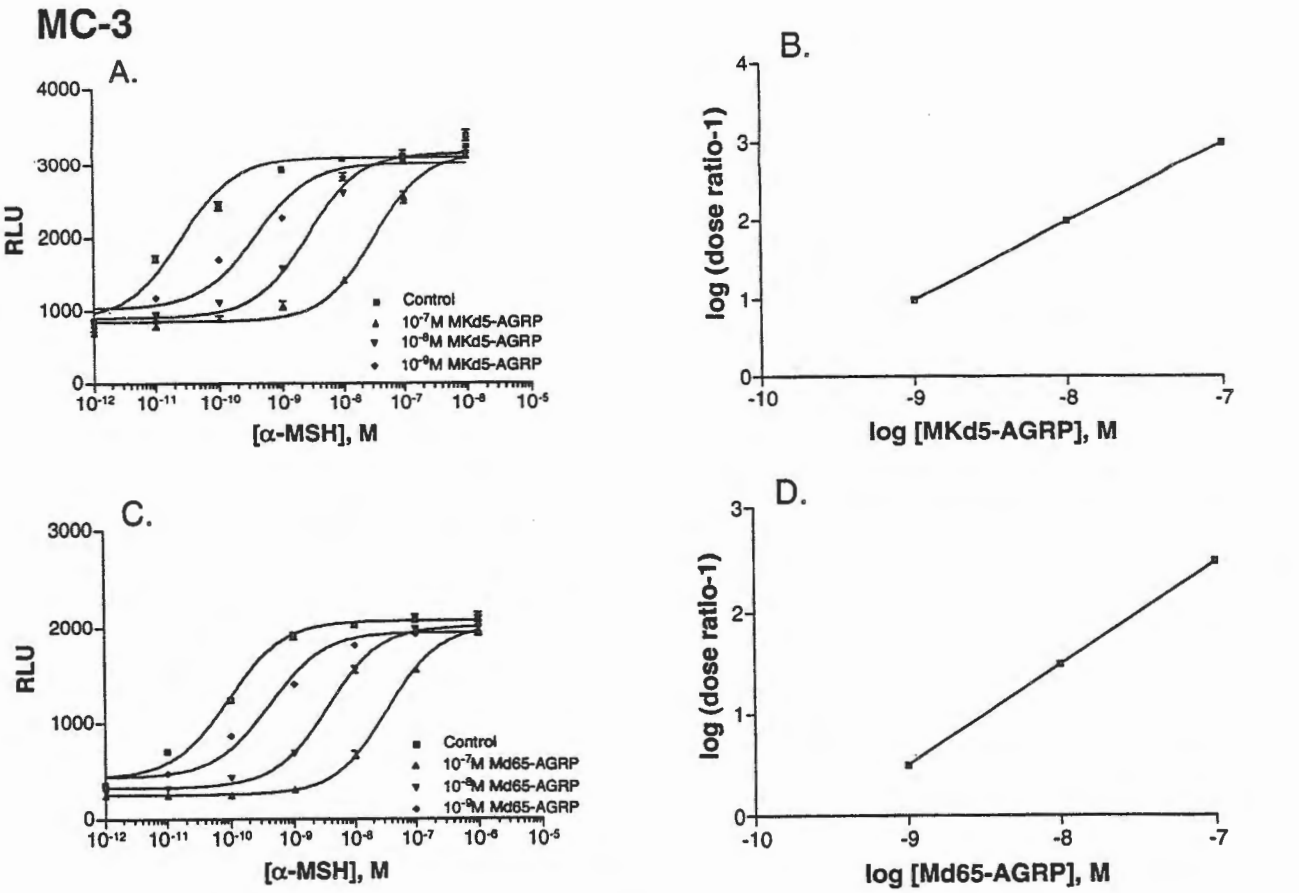

FIGURE 8: Competitive inhibition of α-MSH-stimulated luciferase activity of AGRP proteins in cells expressing MC-3. Measurements of dose responses to α-MSH were taken in the absence (control) or presence of increasing concentrations of either (A) MKd5-AGRP or (C) Md65-AGRP as indicated. Each point represents the mean of triplicate determinations from a single experiment. The respective Schild plots are shown in panels b and d. Repeated experiments yielded comparable results.

(Md65-AGRP), it does recognize a form of AGRP missing the first 28 amino acids (lanes 5 and 12), as well as the intact N-terminal domain (data not shown). Therefore, proteolytic processing that resulted in an intact N-terminal peptide not including the cysteine-rich domain would have been detected. Western blot analysis indicated that AGRP was present in the AtT20 conditioned media at a concentrtion of 2−4 ng/mL, making isolation of AGRP from the conditioned medium impractical.

MC-3 and MC-4 Binding and Functional Studies. The high-affinity radioligand, [^{125}I]NDP-α-MSH, was used to label MC-3 and MC-4, and the affinities (IC_{50}) of these receptors for MKd5-AGRP, Md65-AGRP, and selected reference peptides were determined in competition binding studies. At MC-3, NDP-α-MSH was the most potent compound tested (0.9 nM), followed by Md65-AGRP (2 nM) and MKd5-AGRP (20 nM) (Figure 7). MT II, a cyclic analogue of α-MSH, and HP 228, a heptapeptide analogue, had IC_{50} values of 20 and 117 nM, respectively. α-MSH was the least potent compound tested (250 nM). At MC-4, NDP-α-MSH (7 nM) and MT II (7 nM) were equipotent, whereas Md65-AGRP (19 nM), HP 228 (33 nM), and MKd5-AGRP (88 nM) were somewhat less potent (Figure 7). As seen at MC-3, α-MSH (550 nM) was the least potent compound tested at MC-4. Competition curves were consistent with a noninteracting, single-site receptor model.

In the cell-based functional assay, both MKd5-AGRP and Md65-AGRP were found to be competitive inhibitors of α-MSH-stimulated cyclic AMP production measured as luciferase activity in both MC-3 and MC-4 cell lines. In the absence of AGRP proteins, α-MSH was somewhat more potent at MC-3 than at MC-4. To determine the antagonist potencies of MKd5-AGRP and Md65-AGRP, experiments for determining dose responses to α-MSH were performed in the presence of multiple, fixed concentrations of AGRP proteins. Both AGRP proteins produced a parallel, rightward shift in the α-MSH dose−response curve at MC-3 and MC-4, consistent with competitive antagonism (Figures 8 and 9). Linear regression analysis of the transformed data (Schild regression) was used to determine pA_2 values for each AGRP protein. MKd5-AGRP was slightly more potent at MC-3 ($pA_2 = 10.0$) than at MC-4 ($pA_2 = 9.5$), whereas Md65-AGRP was equipotent at MC-3 and MC-4 ($pA_2 = 9.5$) (Figures 8 and 9). Since the pA_2 is equal to $-\log K_{DB}$, a pA_2 value of 10.0 is equal to an antagonist affinity of 0.1 nM. In all cases, the slope of the Schild plot was not significantly different from 1.0, again consistent with the notion that these compounds are competitive inhibitors of α-MSH. To assess the specificity of action, both AGRP proteins were tested for their ability to inhibit cAMP production at MC-1 and MC-5. Neither form of AGRP produced inhibition at these melanocortin receptor subtypes at concentrations up to 1 μM (data not shown), demonstrating their selectivity for MC-3 and MC-4.

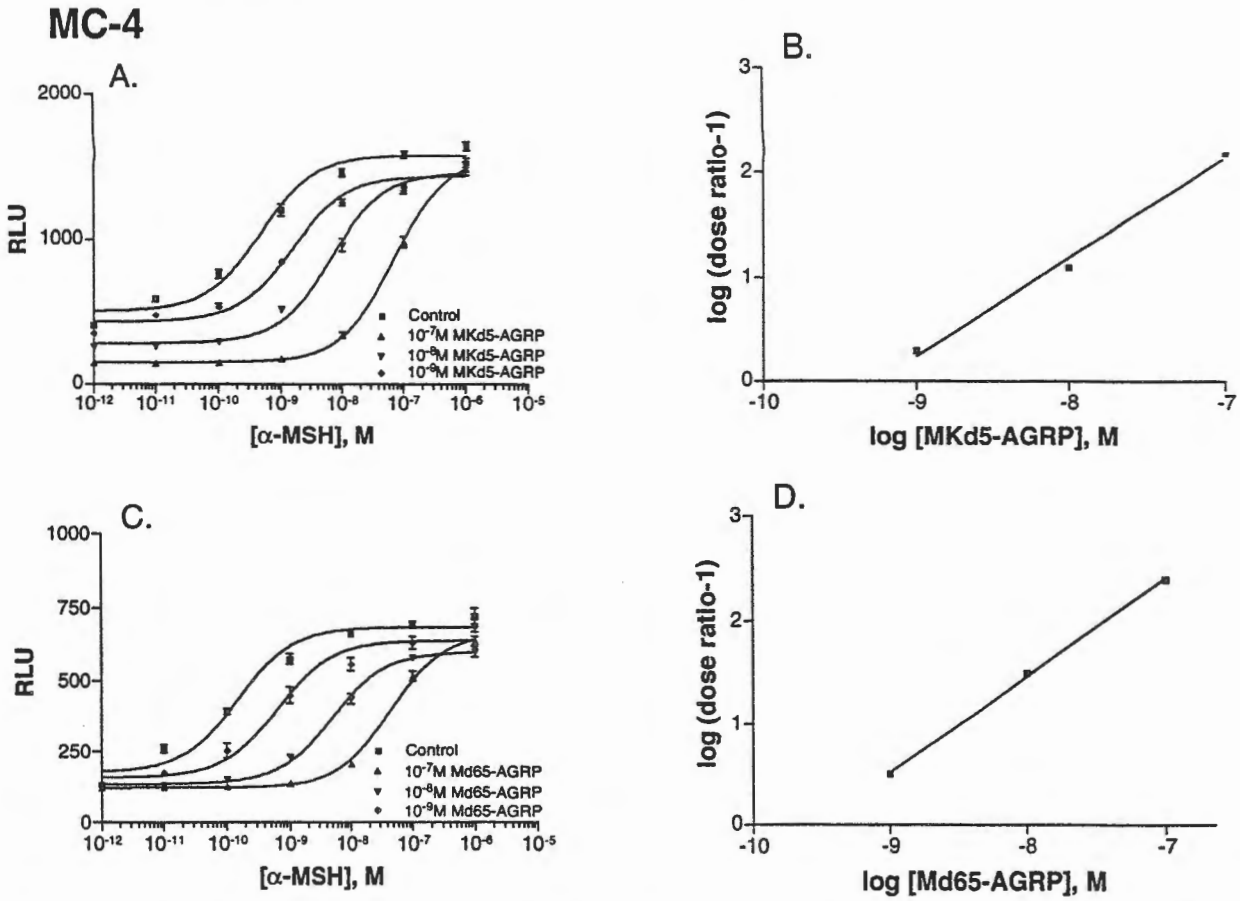

FIGURE 9: Competitive inhibition of α-MSH-stimulated luciferase activity of AGRP proteins in cells expressing MC-4. Measurements of dose responses to α-MSH were taken in the absence (control) or presence of increasing concentrations of either (A) MKd5-AGRP or (C) Md65-AGRP as indicated. Each point represents the mean of triplicate determinations from a single experiment. The respective Schild plots are shown in panels b and d. Repeated experiments yielded comparable results.

DISCUSSION

Studies of agouti as well as AGRP have made use of a baculovirus or COS-7 cell expression system for producing the respective recombinant proteins (*8*, *13*, *14*, *27*). Expression of these proteins utilizing a bacterial expression system has not been described to date. We describe a method for producing, refolding, and purifying two forms of human AGRP using an *E. coli* expression system. Although MKd5-AGRP resided in the soluble fraction of an *E. coli* lysate, it was present as large intramolecular disulfide-bonded aggregates. An oxidation and refolding step was then initiated with the soluble fraction, after which the protein appeared to be fully oxidized and monomeric. CD analysis showed the final product to have a secondary structure consisting of random coil and β-sheet, similar to the spectrum published for agouti (*27*). The region of the protein responsible for the near-UV CD signal is contained in the C-terminal portion of the molecule, as the C-terminal peptide Md65-AGRP accounted for all of the spectrum seen with MKd5-AGRP. This suggests that the N-terminal 65 amino acids are located in a part of the protein which is very flexible, with a much less compact structure than the C-terminal portion of the protein. MKd5-AGRP retained native structure at high temperatures, with melting beginning at about 80 °C. It was also stable to acid, with low pH inducing only very slight changes in secondary structure, with a small increase in the amount of α-helix and β-sheet, but not affecting the tertiary structure in the region around the disulfide bonds. This lack of unfolding in the presence of acid has been seen with other proteins and demonstrates that AGRP is a type III protein (*30*).

It was also demonstrated by SDS−PAGE Western blot analysis, carried out under reducing and nonreducing conditions, that AGRP expressed in mammalian AtT20 cells had mobilities identical to that of MKd5-AGRP, an indication of similar disulfide structure. The combination of RP-HPLC, free thiol analysis, and mass spectral analysis indicates that both forms of AGRP are fully oxidized and are folded into a single disulfide structure. The disulfide structure of MKd5-AGRP has recently been determined (*36*) as well as the disulfide structure of Md65-AGRP (Haniu et al., manuscript in progress), showing that the disulfide linkages of the two recombinant AGRP proteins are identical.

Both AGRP proteins were tested for their ability to inhibit cAMP production at MC-1 and MC-5. Neither form of AGRP produced inhibition at these melanocortin receptor subtypes at concentrations up to 1 μM, demonstrating their selectivity for MC-3 and MC-4. The potent binding properties and functional antagonism of MKd5-AGRP at MC-3 and MC-4 are a strong indication that the protein is correctly oxidized and properly folded. Likewise, Md65-AGRP was also functionally active, consistent with the finding (*27*) that the C-terminal portion of agouti also retains full biological activity. Interestingly, we observed a tendency for AGRP to reduce basal cAMP production in cells expressing MC-4, but not MC-3. This finding was noted in other human MC-4

clonal cell lines, as well as in one cell line expressing rat MC-4 (data not shown). Ollmann et al. (*13*) also noted a reduction in basal cAMP levels in response to partially purified AGRP in MC-4-transfected cells. However, the maximum response to α-MSH was also greatly reduced in these cells, an effect that we have not observed. It is conceivable that MC-4 exhibits some low level of constitutive activity under the conditions that we used in this study, and that AGRP inhibits this activity.

Regardless, both MKd5-AGRP and Md65-AGRP are competitive inhibitors of α-MSH at MC-3 and MC-4 in vitro, supporting the notion that AGRP functions in vivo to regulate neuronal melanocortinergic activity. The obesity and diabetes observed in mice overexpressing AGRP (*12*, *13*) are likely due to chronic blockade of central melanocortin receptors. The presence of unique features of the obese phenotype (e.g., normal corticosterone levels and increased linear growth) observed in mice lacking the MC-4 (*10*), and overexpressing agouti (*35*) or AGRP, further suggests a common mechanism between these animal models of obesity. This would further imply that ectopic expression of agouti causes obesity by mimicking the normal role of AGRP expressed within the brain. Since the expression pattern of AGRP, unlike agouti, is the same in rodents and humans, it is probable that both species use this protein to control the same signaling pathways (*11*).

The availability of highly purified recombinant protein as described here allows further avenues of research. For example, administration of AGRP to rodents would allow a determination of the behavioral effects of defined doses of this protein, in both normal and mutant backgrounds. The available data suggest that a compound that selectively inhibits AGRP binding to melanocortin receptors could be a useful anti-obesity agent in humans. The ability to generate large quantities of highly purified protein will enable the development of high throughput screening assays for identifying molecules that disrupt AGRP binding to melanocortin receptors.

ACKNOWLEDGMENT

We thank Tsutomu Arakawa and Keith R. Westcott for helpful discussions with the manuscript, Joan Bennett for help in preparing the manuscript, and Danette Baron for her excellent graphics support.

REFERENCES

1. Zhang, Y., Proenca, R., Maffei, M., Barone, M., Leopold, L., and Friedman, J. M. (1994) *Nature 372*, 425.
2. Naggert, J. K., Frisker, L. D., Varlamov, O., et al. (1995) *Nat. Genet. 10*, 135−142.
3. Noben-Trauth, K., Naggert, J. K., North, M. A., and Nishina, P. M. (1996) *Nature 380*, 534−538.
4. Kleyn, P. W., Fan, W., Kovats, S. G., et al. (1996) *Cell 85*, 281−290.
5. Cuenot, L. (1905) *Arch. Zool. Exp. Gen. 3*, 123−132.
6. Manne, J., Argeson, A. C., and Siracusa, L. D. (1995) *Proc. Natl. Acad. Sci. U.S.A. 92*, 4721−4724.
7. Bultman, S. J., Michaud, E. J., and Woychik, R. P. (1992) *Cell 71*, 1195−1204.
8. Lu, D., Willard, D., Patel, I. R., Kadwell, S., Overton, L., Kost, T., Luther, M., Chen, W., Woychik, R. P., Wilkinson, W. O., and Cone, R. D. (1994) *Nature 371*, 799−802.
9. Fan, W., Boston, B. A., Kesterson, R. A., Hruby, V. J., and Cone, R. D. (1997) *Nature 385*, 165−168.
10. Huszar, D., Lynch, C. A., Fairchild-Huntress, V., Dunmore, J. H., Fand, Q., Berkmeier, L. R., Boston, B. A., Cone, R., Smith, F. J., Campfield, L. A., Burn, P., and Lee, F. (1997) *Cell 88*, 131−141.
11. Shutter, J. R., Graham, M., Kinsey, A. C., Scully, S., Lüthy, R., and Stark, K. L. (1997) *Genes Dev. 11*, 593−602.
12. Graham, M., Shutter, J. R., Sarmiento, U., Sarosi, I., and Stark, K. L. (1997) *Nat. Genet. 17*, 274.
13. Ollmann, M. M., Wilson, B. D., Yang, Y.-K., Kerns, J. A., Chen, Y., Gantz, I., and Barsh, G. S. (1997) *Science 278*, 135−138.
14. Fong, T. M., Mao, C., MacNeil, T., et al. (1997) *Biochem. Biophys. Res. Commun. 237*, 629−631.
15. Laemmli, U. K. (1970) *Nature 227*, 680−685.
16. Towbin, H., Staehelin, T., and Gordon, J. (1979) *Proc. Natl. Acad. Sci. U.S.A. 76*, 4350−4354.
17. Philo, J. S. (1997) *Biophys. J. 72*, 435.
18. Laue, T. M., Shah, B. D., Ridgeway, T. M., and Pelletier, S. L. (1992) in *Analytical ultracentrifugation in biochemistry and polymer science* (Harding, S. E., Rowe, A. J., and Horton, J. C., Eds.) pp 90−125, Royal Society of Chemistry, Cambridge, U.K.
19. Bradford, M. M. (1976) *Anal. Biochem. 72*, 248−254.
20. Ellman, G. L. (1959) *Arch. Biochem. Biophys. 82*, 70−77.
21. Arunlakshan, O., and Schild, H. O. (1959) *Br. J. Pharmacol. 14*, 48−58.
22. Stempfer, G., Neugebauer, B. H., and Rudolph, R. (1995) *Nat. Biotechnol. 14*, 329−334.
23. Shoemaker, J. M., Brasnett, A. H., and Marston, F. A. O. (1985) *EMBO J. 4*, 775−780.
24. Hober, S., Forsberg, G., Palm, G., Hartmanus, M., and Nilsson, B. (1992) *Biochemistry 31*, 1749−1756.
25. Langley, K. E., Lai, P. H., Wypych, J., Everett, R. R., Berg, T. F., Krabill, L. F., and Souza, L. M. (1987) *Eur. J. Biochem. 163*, 323−330.
26. Chang, C. T., Wu, C.-S. C., and Yang, J. T. (1978) *Anal. Biochem. 91*, 13−31.
27. Willard, D. H., Bodnar, W., Harris, C., Kiefer, L., Nichols, J. S., Blanchard, S., Hoffman, C., Moyer, M., Burkhart, W., Weiel, J., Luther, M. A., Wilkison, W. O., and Roque, W. J. (1995) *Biochemistry 34*, 12341−12346.
28. Narhi, L. O., Philo, J. S., Li, T., Zhang, M., Samal, B., and Arakawa, T. (1996) *Biochemistry 35*, 11454−11460.
29. Gast, K., Damaschun, H., Eckert, K., Schulze-Forster, K., Maurer, H. R., Muler-Frohne, D. Z., Czarnecki, J., and Damaschun, G. (1995) *Biochemistry 34*, 13211−13218.
30. Fink, A. L., Calciano, L. J., Goto, Y., Karotsu, T., and Pallaro, D. R. (1994) *Biochemistry 33*, 12504−12511.
31. Eipper, B. A., and Mains, R. E. (1976) *Endocr. Rev. 1*, 1−27.
32. Moore, H. P. H., Walker, M. D., Lee, F., and Kelly, R. B. (1983) *Cell 35*, 531−538.
33. Nagahama, M., Nakayama, K., and Murakami, K. (1991) *Eur. J. Biochem. 197*, 135−140.
34. Dickerson, I. M., Dixon, J. E., and Mains, R. E. (1987) *J. Biol. Chem. 262*, 13646−13653.
35. Klebig, M. L., Wilkinson, J. E., Geisler, J. G., and Woychik, R. P. (1995) *Proc. Natl. Acad. Sci. U.S.A. 92*, 4728−4732.
36. Bures, E. J., Hui, J. O., Young, Y., Chow, D. T., Katta, V., Rhode, M. F., Zeni, L., Rosenfeld, R. D., Stark, K. L., and Haniu, M. (1998) *Biochemistry* (in press).

BI981027M